Mem. S.A.It. Vol. 95, 77

Memorie della

Spectroscopy of cosmic dust by "space tweezers", a review

A. Magazzù[1], D. Bronte Ciriza[1,2], A. Musolino[3,4], S. Ferretti[3,4] S. Marrara[1,2], A. Mandanici[2], M. G. Donato[1], A. Foti[1], P. G. Gucciardi[1], M. A. Iatì[1], R. Saija[2], V. Della Corte[3], A. Jimenez Escobar[5], C. Cecchi-Pestellini[5], A. Ciaravella[5], A. Rotundi[4]

[1] CNR-IPCF, Istituto per i Processi Chimico-Fisici, I-98158, Messina, Italy
[2] Dipartimento di Scienze Matematiche e Informatiche, Scienze Fisiche e Scienze della Terra, Università di Messina, Italy
[3] INAF-IAPS, Istituto Nazionale di Astrofisica, Istituto di Astrofisica e Planetologia Spaziali, Rome, Italy
[4] Dipartimento di Scienze e Tecnologie, Università degli studi di Napoli Parthenope, Italy
[5] INAF-OAPa, Osservatorio Astronomico di Palermo, Palermo, Italy e-mail: alessandro.magazzu@cnr.it

Received: 26 March 2024; Accepted: 26 June 2024

Abstract. Optical tweezers, tools based on focused laser beams, enable trapping, manipulation, and characterization of a wide range of microscopic and nanoscopic particles, in liquids, air, and vacuum. Key applications of this contactless technique have been developed in many fields. Despite this progress, applications to planetary exploration and cosmic dust characterization have been only partially considered. The "space tweezers" project aimed to develop research activities based on optical and acoustic trapping methods to confine and characterize spectroscopically extraterrestrial particles and their analogs. This opened opportunities to apply optical and, acoustic fields for the trapping and manipulation of particulate matter at the sub-millimeter scale paving the way for more challenging applications such as in situ analyses or contactless characterization of dust from sample-return missions.

Key words. Cosmic dust — Optical trapping — Raman tweezers — Acoustic tweezers

1. Introduction

With the advent of astrophysical sciences and its related technology (space missions, optical and radio telescopes), cosmic dust has bloomed the interest of scientists due to its role in the universe. Cosmic dust is a comprehensive term indicating small solid particles with sizes ranging from a few nanometers to hundreds of micrometeres. They float in the interstellar medium or in the interplanetary space in the solar system. Interstellar dust is mainly generated by the lifecycles of many generations of stars. It is released by radiation pressure and solar wind or ejected during the gigantic supernova explosions or during the blowing off of the novae outer layers (Woosley & Weaver, 1995; Woosley

et al., 2002; Calura et al., 2008; Brownlee, 2016). Stardust, literally dust formed around stars, is not the same as interstellar dust, and must be regarded as the feedstock from which true interstellar dust is formed (Draine et al., 2009; Brownlee, 2016). Interplanetary dust consists of small solid particles generated by collisions between solid bodies (e.g., asteroids, planets, and their satellites) or evaporation of icy bodies (e.g., comets) (Rietmeijer, 1998). While interstellar dust is almost exclusively analysed through remote, mainly spectroscopic, observations (Draine, 2003; Lodders & Amari, 2005; Brownlee, 2016), interplanetary dust is available in our laboratories, through sample-return space missions (Westphal et al., 2014; Brownlee et al., 2003; Frank et al., 2014), collections in the Earth's stratosphere (Testa Jr et al., 1990; Taylor et al., 1996; Lauretta et al., 2017; Della Corte et al., 2012; Brownlee, 1985) or at the Earth's surface in the form of micrometeorites (e.g., (Genge et al., 2008; Folco et al., 2015; Taylor et al., 2016; Brownlee, 1985)). Planetary dust is also a major component of the in situ surface sampling of planetary surfaces by current and future sample-return space missions (e.g., JAXA Hayabusa 2 to asteroid 162173 Ryugu; NASA OSIRIS-REx to asteroid 101955 Bennu; etc. (Watanabe et al., 2019; Lauretta et al., 2022)). Samples are analysed at terrestrial facilities by state-of-the-art analytical techniques—since the size of some instruments is still too large to fly to the space (Rietmeijer, 2001; Rauf et al., 2010; Della Corte et al., 2014). Here we review some of the results of the "Space Tweezers" project where we investigate optical and acoustic trapping and optical forces on dust particles and their potential to characterize single grains by spectroscopic methods, Fig. 1. We discuss how Raman tweezers enable the identification of mineral and organic compositions of cosmic dust grains, searching for biogenic signatures.

2. Samples selections

To test the trapping and spectroscopic characterization of cosmic dust by optical tweezers, we first selected four different terrestrial and extraterrestrial samples having a well known mineral composition. In particular the terrestrial rock samples are a quartzarenite from Kamil Crater in Egypt (M26) (Fazio et al., 2014) and a hawaiite from Etna volcano in Italy (HE-1). The extraterrestrial samples are the CV3-OxA carbonaceous chondrite Allende meteorite (A-1), and a lunar meteorite (polymict regolith breccia) found in Antarctica (DEW 12007) (Collareta et al., 2016). Previously, mineral grains used to calibrate the dust analyser Giada on board of Rosetta space mission (Colangeli et al., 2007) were used as the simplest possible starting material (monomineralic, uniform size range). The two terrestrial rock samples M-26 and HE-1 have been chosen due to their complex non-uniform mineral composition and texture considered inasmuch analogues of mono- and polymineralic planetary materials while the two extraterrestrial rocks as representative of primitive (A-1) and differentiated (DEW 12007) bodies of the solar system.

3. Spectroscopic characterisation in optical tweezers

The collected cosmic dust is mainly analysed as an aggregation of single micron sized particles (apart few exceptions (Alali et al., 2020; Abbas et al., 2007) by different techniques, making the characterisation of a single grain quite difficult. Usually the dust is deposited on a substrate and collective and averaged physico-chemical properties are studied by X-rays to get general information (Mackinnon & Rietmeijer, 1987), SEM and TEM for the mineralogical composition (Lewis et al., 1987), IR and Raman spectroscopy to identify minerals and organic compositions (Rotundi et al., 2008; Davidson et al., 2012) and mass spectroscopy to study the isotopic and mineralogical composition of cosmic dust samples (Floss et al., 2006). Recent studies allowed the detection and characterization of nanometer-sized particles (less than 20 nm), such as ultrafine cosmic dust, with novel methods based on plasmon-enhanced spectroscopies (Huck et al., 2019). However, these techniques may induce shielding effects by the substrates or by other

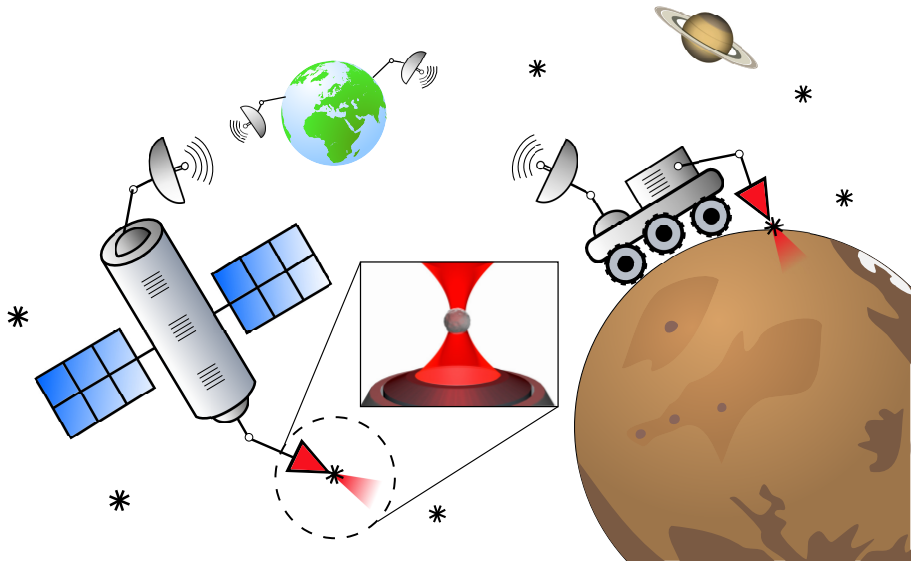

Fig. 1. Pictorial representation of the space tweezers project, where interplanetary or planetary dust can be collected and investigated directly in open space or extraterrestrial surfaces, and only analysed data are sent to our planet. The inset represents a closeup of a grain of interplanetary dust trapped by single-beam optical tweezers. Reproduced under Creative Commons license (Polimeno et al., 2018).

particles. To overcome these unwanted effects we use optical and Raman tweezers, which are contactless and non-destructive techniques, to manipulate and investigate single dust grains without the shielding effects of any substrate or other particles.

For the investigations of cosmic dust in liquid we used standard optical tweezers and Raman tweezers setups (Polimeno et al., 2018). These setups are powerful tools based on the non-invasive optical trapping technique, which allows us to trap and manipulate single nanometer and micron-sized objects by a high focused laser beam, without any physical contact (Ashkin et al., 1986; Magazzú et al., 2015; Jones et al., 2015). All the samples are provided as dried powder having a non homogeneous size and shape distribution, as shown in Fig. 2a. Powder samples are then dispersed in water by ultrasound sonication at an appropriate concentration for optical trapping (e.g. few particles / μl) and the sample solution is placed in a glass cavity slide and sealed by a coverglass, as shown in Fig. 2(b,c).

In particular, for the investigation of single-grain dust particles we used two different customised setups: a standard optical tweezers and a Raman tweezers (Gillibert et al., 2019; Magazzù et al., 2022). Our standard optical tweezers have a laser diode source generating a linear polarised laser beam with a wavelength of 830 nm. The output laser beam is expanded by a two lenses telescope system and reflected by a dichroic mirror in order to overfill the back aperture of a 100X oil immersion objective with a high numerical aperture (NA=1.3). This objective is used to achieve a high focus of the laser beam and to image the sample. The overfilling creates a maximal optical field gradient at the focal spot, resulting in more efficient optical trapping. This occurs when the gradient forces, which always point toward the focal spot, overcome the scattering forces that push the particle along the laser propagation direction, destabilizing the trapping process. A sample holder is equipped with a 3D translation stage to move the focal spot within the cavity glass slide containing the sample solu-

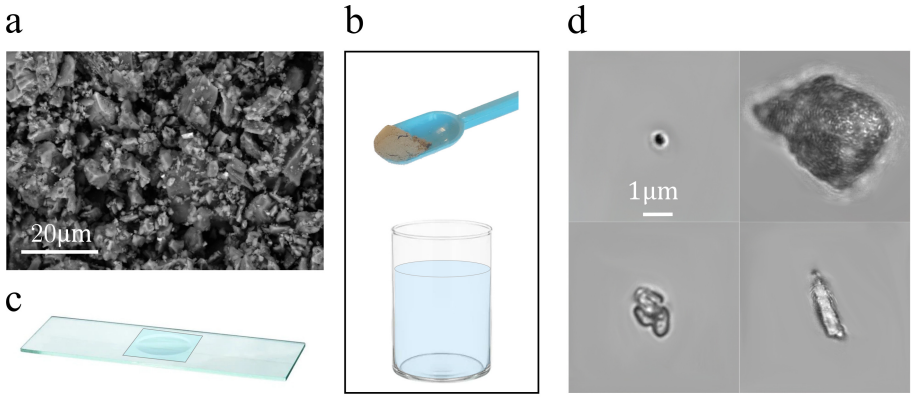

Fig. 2. Samples preparation. a) SEM image of the lunar meteorite (DEW 12007), where it is possible to notice its granular composition. b) Dust samples are dispersed in water by ultrasound sonication and c) this solution is placed within a cavity glass slide, sealed by a coverglass. d) Screenshots of four different 3D optically trapped grains of cosmic dust in water solution having different size and morphology. Reproduced under Creative Commons license (Magazzù et al., 2022).

tion. The dichroic mirror used to reflect the laser beam to the objective acts like a short pass filter, it reflects the laser light and transmits the visible light to a CMOS camera, preventing the saturation of the detector and allowing to view of the sample on a monitor. The polarisation of the trapping beam can be changed by a waveplate to investigate the optical response of cosmic dust at different light polarisation. In particular, changing the light polarisation from linear to circular right or left we can investigate the occurrence of spin-angular angular momentum transfer from light to the dust (Donato et al., 2014; Jones et al., 2015; Magazzù et al., 2022). Forward scattered light from a trapped particle contains information about the position of a trapped particle. In particular, the superposition of the scattered and transmitted light is collected by a condenser, producing an interferometric pattern, which is reflected by a second dichroic mirror on a quadrant photo diode (QPD) (Polimeno et al., 2018; Jones et al., 2015). A QPD converts the interferometric pattern collected by a condenser in analogical voltage signals, proportional to the displacement of the particle from its equilibrium position, (Gittes & Schmidt, 1998; Jones et al., 2015). These signals can be analysed by a PC to rebuild the 3D position and eventually rotations of the trapped particle, providing information about the effects of light on a single grain of cosmic dust (Gieseler et al., 2021; Irrera et al., 2016; Magazzù et al., 2022; Donato et al., 2016, 2014). The Raman tweezers used for the identification of the minerals in our samples is a customised setup obtained by coupling a customized optical tweezers with a commercial Raman spectrometer (Horiba TRIAX 190) by a notch filter. This filter reflects the laser light to the back aperture of the objective, similarly to the dichroic mirror in the standard optical tweezers setup, but instead of being a short pass filter as the dichroic, it reflects only the single wavelength of the laser beam, and it is transparent to the other ones. In such a way, only the elastic component of the scattering is cut out by the notch filter, that transmits only the Raman component to the spectrometer, which is equipped with a grating giving a spectral resolution of 8 cm^{-1}, and coupled to a silicon Peltier-cooled CCD camera. To excite the Raman signal from our trapped samples, we used a linearly polarized laser with a wavelength of 785 nm. All the selected samples were trapped and analysed optomechanically. The HE-1 Etna, M26

Kamil, DEW12007 samples were successfully and stably trapped in three dimensions, while the Allende sample (A-1) was confined only in 2D, due to the strong absorption of light (probably due to one of its components), showing a strong radiation pressure component which destabilized the single-beam trap. We observe that for both terrestrial and extra-terrestrial samples, optically trapped by linear polarised light, the stiffness of the optical trap increases as the laser power. In particular in Fig. 3a is shown the stiffness of a single trapped grain of regolith from the lunar meteorite DEW12007. In Fig. 3a the stifnesses k_x, k_y and k_z increase linearly with the laser power and the difference between the k_x, k_y values is due to an eventual break of the system symmetry around the propagation axis z possibly due to an asymmetry of the sample. Usually the values of the stiffness K_z are lower than the values of k_x and k_y because the radiation pressure pushes and destabilize the particle along the z direction. It is noteworthy that the shape of the particles can play an important role in the light - particle interaction. In the case of asymmetric particles, light can exert a mechanical torque on the particles inducing rotations as shown in Fig. 3b. In particular, we observe that the rotational frequencies of three different trapped samples increase as the laser power, Fig. 3b.

Rotations induced by linear polarised light are due only to the mechanical torque exerted by the light on the particles since linear polarised light (LP) does not carry any spin-angular momentum. In the case of polarised light, rotations of the trapped particles can occur whenever there is a spin angular transfer from the laser beam to the sample, as shown in Fig. 3c for a grain of HE-1 from Etna. In this case, rotations are due to the sum of two contributes: the mechanical torque and the transfer of spin-angular momentum. It is noteworthy that mechanical torque depends on the shape of the particle, while the transfer of spin-angular momentum depends on the absorption properties of the particle (Donato et al., 2016, 2014). Therefore, the total opto- mechanic interaction of particle with light, depends on both the particle shape and the polarisation of the laser beam. In Fig. 3c the rotational frequency Ω_{tot} of an optically trapped grain of the terrestrial samples HE-1-Etna is shown for different light polarisation. Here Ω_{tot} decreases from -18 s^{-1} for LCP to -28 s^{-1} for RCP with a central value of -23 s^{-1} for LP indicating that the trapped particle is absorbing circular polarised light with a spin angular momentum $+\hbar$ for left circularly polarised light (LCP) and $-\hbar$ for right circularly polarised light (RCP). Thus, negative frequency values mean a rotation anticlockwise with respect to the z axis, while positive frequency values mean a rotation clockwise with respect to the z axis. The rotational frequency Ω_{tot} due to the radiation pressure torque, for LP light is -23 s^{-1}, while the spin angular momentum torque sums or subtracts depending on the helicity of light (Donato et al., 2016, 2014).

Spectroscopic analysis of individual single grains was carried out by Raman tweezers and in Figure 4a, we report a Raman spectrum (black line) collected from a single optically trapped grain of sample M26. According to the literature, the sample mainly contains quartz whose reference spectrum is represented by the red line. Similarly, in Figure 4b, we report the Raman spectra of a single grain of sample HE-1 from Etna volcano (black line) and of A-1 from the Allende meteorite (blue line). Both the Allende meteorite and the basalt from Etna show a Raman signaure of Mg-olivine, one of their main consitutent phases accordng to literature. Good agreement with reference spectra of the consitutent phases of our samples have been observed in all the experimental run on a variey of particles.

After testing our Raman tweezers on terrestrial dust sample, we started a systematic study for the lunar regolith sample DEW12007 by trapping approximately 70 different grains and following a precise spectra acquisition and analysis protocol. For each trapped particle, in addition to its spectrum, a reference spectrum without particles is acquired to remove the background signal (due to water, glass, objective immersion oil). Then, through a fitting routine, the main peaks for each sample are identified and compared with reference spectra in the literature for mineralogical analysis (Collareta et al., 2016). In Figure 5(a-d) four spectra of

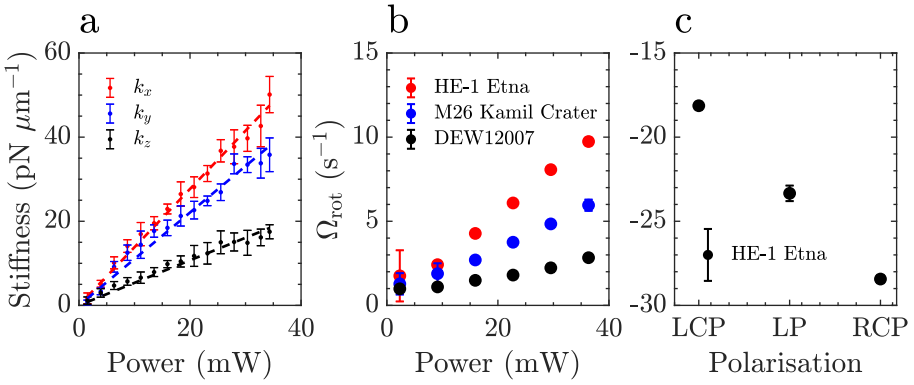

Fig. 3. Effects of the laser power and polarisation on trapped particles. a) Trap stiffnesses (harmonic approximation, i.e., $F_x = -\kappa_x x$ for a trapped dust grain of the lunar meteorite DEW12007 as function of the power measured at the objective. b) Particle rotation as function of the laser power measured at the objective for different trapped grains. c) Rotational frequencies of optically trapped single dust grains of HE-1 from Etna, in presence of left circular polarised (LCP), linear polarised (LP) and right circular polarised (RCP) light. The rotational frequencies change due to the transfer of angular momentum of spin for right-handed (RCP) or left-handed (LCP) circularly polarized light. The spin angular momentum is added or subtracted from the angular momentum induced by the shape of the grain for the "windmill effect". Reproduced under Creative Commons license (Magazzù et al., 2022).

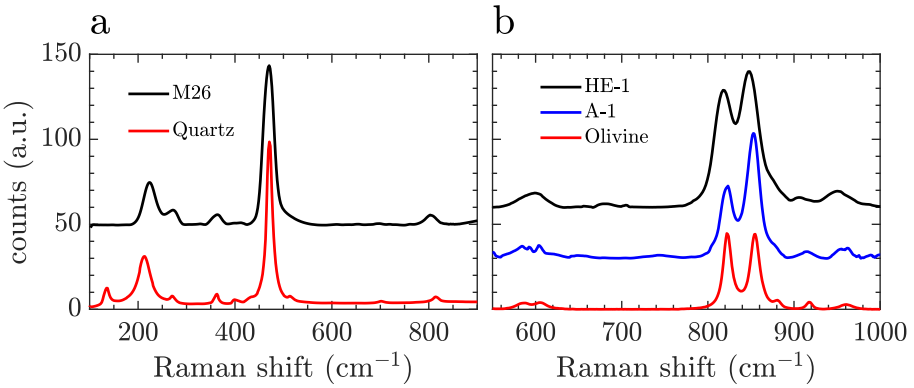

Fig. 4. Raman spectra of individual dust grains trapped in the Raman tweezers. a) M26 from Kamil crater (black line); the red line represents the Raman spectrum of the quartz used as reference (RRUFF R150074). b) HE-1 from Etna (black line), and A-1 from Allende meteorite (blue line). The red line represents the Raman spectrum of the olivine of intermediate composition used as a standard reference (RRUFF X050088). All spectra have been shifted on the vertical axis for clarity and the background spectra acquired without any trapped particle were subtracted to eliminate any signal contributions from oil, glass, and water. Reproduced under Creative Commons license (Magazzù et al., 2022)

.

four different grains optically trapped of the DEW12007 lunar regolith are shown (black lines). Each single trapped grains contains only a single mineral component, among the sev-

eral ones reported in literature, as shown by the match with the reference spectra (coloured lines). We identified also polymineralic single grains Fig. 5e, as expected for a rock in which the grain size is highly variable. From the analysis of the Raman spectra of 70 different grains it is therefore possible to determine the occurrence of the different minerals in the DEW12007 lunar regolith as shown in Fig. 5f, which are consistent with the dominant mineralogical composition on the surface of the Moon. It is noteworthy that we did not change the polarization of the beam during our spectroscopic investigation, which resulted in no transfer of linear or angular momentum to the particle. Also, in the case of rotations induced by the "windmill effect" due to the scattering of incident photons on a possibly irregular particle surface, we expect that the acquired Raman spectrum does not depend on these rotations. This is because optically trapped micro-objects are located around the center of the focal spot, whose size is usually in the same range as the particle size. The laser spot is typically less than one micrometer, and the dimensions of trapped particles can range from fractions of a micrometer to a few micrometers. Additionally, our acquisition times are usually longer than the typical rotation periods of trapped microparticles.

Cosmic dust can be investigated also in vacuum, which is a more native environment than water avoiding any possible interaction and reaction of the sample with water. Trapping in air/vacuum and water are very similar, the trapping mechanisms are the same and the major difference is that the buoyancy is negligible in air since air density is 1000 times less than that of water. This makes optical trapping of microparticles in vacuum or air much more difficult than trapping in water because we have to launch or nebulize many particles in order to trap one of them passively. Conversely, in water we can actively search for specific micro particles suspended in the medium by moving the sample chamber. Furthermore, in air, whenever a particle escapes from the optical trap it falls immediately down due to gravity and it is lost forever, while in water it remains suspended in the medium near the trapping region (Gong et al., 2018).

4. Modelling optical forces on cosmic dust particles

Optical forces are the result of mechanical effects of light on particles, which are a consequence of the conservation of linear and angular electromagnetic momentum during a scattering process (Jones et al., 2015). The scattering of electromagnetic waves by spherical particles can be obtained by Mie theory, while the scattering by non-spherical or non-homogenous particles requires the full electromagnetic theory based on the Maxwell's equations (Mishchenko et al., 2002) and the integration of the averaged Maxwell stress tensor (Jones et al., 2015; Borghese et al., 2007). However, such calculations can be extremely complex and may require computational intensive procedures, especially for non-spherical or non-homogeneous particles. To overcome such limitation several approximations have been developed for a better understanding and faster calculations of optical forces. The T-matrix method is among the most accurate methods for the calculation of optical forces in the intermediate regime, where the scattering particle size is comparable with the light wavelength λ (Polimeno et al., 2018; Jones et al., 2015). This method consists in a complete wave-optical modelling of the particle–light interaction and is widely used to calculate optical forces. The T-matrix method is also used to calculate the effects of light on inhomogeneous and nonspherical particles, on spheres with spherical (eccentric) inclusions, and multilayered spheres that can be modelled as aggregates of single spherical particles (Borghese et al., 2007; Saija et al., 2003). The T-matrix method is based on the expansion of the incident and scattered plane electromagnetic waves by a single particle, as vector spherical wave functions and relating these expansions by means of a transition matrix (T-matrix), where the elements of the T-matrix contain all the particle information as refractive index, size, shape and orientation with respect to the incident field. The biggest advan-

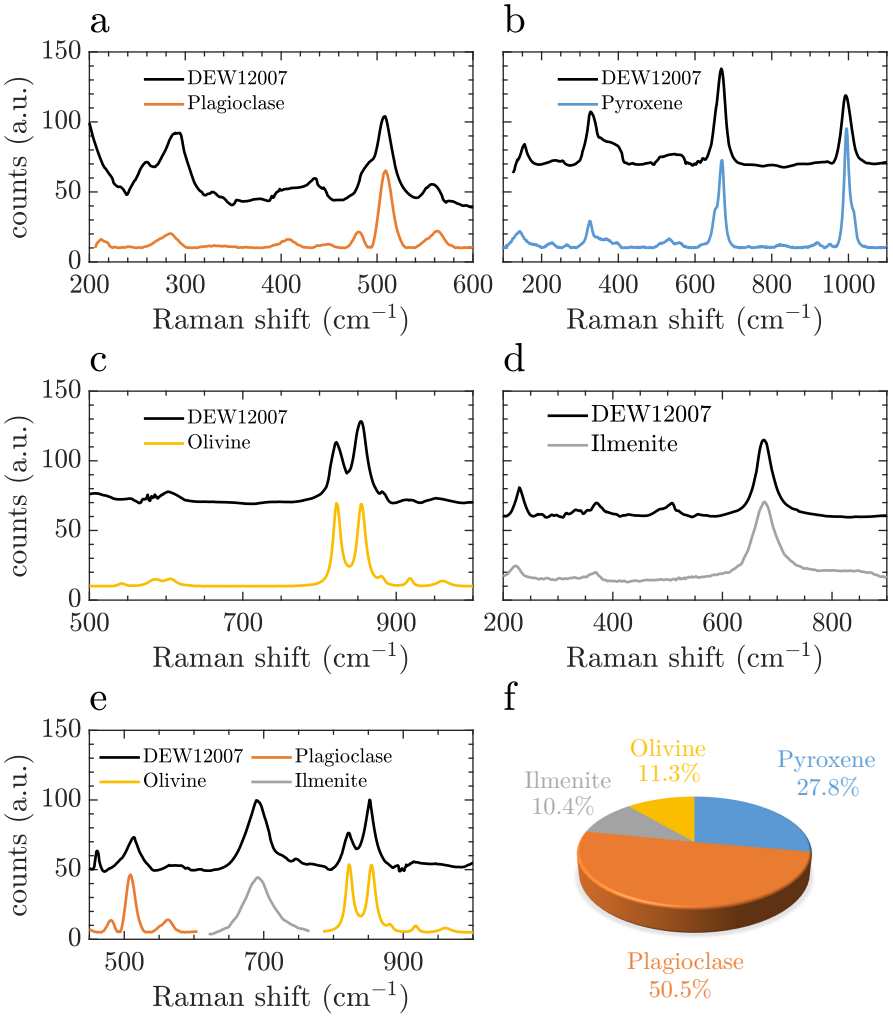

Fig. 5. Raman investigation of the lunar regolith sample DEW12007. a–e) Raman spectra of several lunar regolith grains trapped by Raman optical tweezers. Peaks in the various spectra are identified through fitting routines and compared to reference peaks in the literature to identify the mineralogical composition of the trapped particle. The presence of mineralogical components of Plagioclase, Pyroxene, Olivine, Ilmenite was highlighted. f) Statistical analysis on 70 grains, trapped by Raman optical tweezer. based on the acquired spectra. The analysis reflects the components of the DEW 12007 lunar meteorite. Reproduced under Creative Commons license (Magazzù et al., 2022).

tage of this method is the T-matrix independence from the direction and polarisation of the incident and scattered fields. Once the T-matrix elements are calculated, there is no need to recalculate them if the direction and polarisation of the incident field change (Mishchenko et al., 2002). Thanks to the flexibility and accuracy of this technique, it is possible to theoretically investigate several systems and configurations, making this method ideal for the

investigation of optical forces on cosmic dust (Saija et al., 2001; Iatì et al., 2004, 2008; Saija et al., 2005). To calculate realistic optical forces for space tweezers applications, we used models, like homogeneous and stratified single/aggregated spheres to consider the diversity of dust particles in an astrophysical context, Fig. 6 (Polimeno et al., 2021). In the left column of Figure 6 are reported the extinction cross sections σ_{ext} of the particles for the visible and near-infrared wavelength spectrum. The extinction cross sections σ_{ext} indicates the rate at which the energy is removed from the electromagnetic wave through scattering and absorption and is helpful to understand how effectively trapping takes place, where relatively low σ_{ext} values indicate better trapping (Jones et al., 2015). In the middle column of Figure 6 are reported the optical forces calculated in water, having a refractive index $n_{\text{m}} = 1.33$, with an objective NA = 1.3, while in the right column are reported the optical forces calculated in air or vacuum $n_{\text{m}} = 1$ with NA = 0.9. Usually, for a given particle, optical trapping is more stable in water due to the overdamped viscous dynamics in the fluid, than in air or vacuum where the underdamped dynamics might be more critical for stability (Svak et al., 2018). Furthermore, due to the higher NA in water the equilibrium position ($F = 0$) along the z direction is closer to the nominal focus than in air. The dielectric particles models like the melt silica Fig. 6(h, i), the carbonate cluster Fig. 6(k, l) and even the interstellar dust model of a sphere aggregate Fig. 6(e, f) can be stably trapped (Polimeno et al., 2021). Conversely, the interstellar model particles of a dust sphere Fig. 6b, c, or the Fe–Mg sphere Fig. 6(n, o), show that trapping is not possible neither in water nor in air due to their strong absorption (Polimeno et al., 2021). Whenever the scattering particle size is larger than λ optical forces can be calculated using the geometrical optics (GO) approximation. With this method the incident light beam is discretized into a set of rays and optical forces are computed as the momentum exchanged between the rays and the particle. However, the accuracy of this method increases with the number of rays decreasing the calculation speed and a proper trade-off between accuracy and calculation speed is always required (Jones et al., 2015; Bronte Ciriza et al., 2022). Recently, to overcome this limitations, neural networks were employed to calculate optical forces in a faster and more accurate way (Bronte Ciriza et al., 2022).

5. Acoustic tweezers

In analogy to the trapping forces in optical tweezers, acoustic forces can also be used to confine and manipulate particles. In this case the trapped particles can have dimensions in the order of millimetres, opening new perspectives for the realisation of combined acoustic and optical fields. In our laboratory we have built two acoustic tweezer setups. A first setup is based on an array of transducers (Marzo et al., 2015; Marrara et al., 2023) that allows the 3D manipulation of levitated particles. Trapping is achieved by the interference of the acoustic waves produced by each transducer. Furthermore, by varying the phase of the signals sent to the transducers, it is possible to change the total acoustic field in real time, allowing particle manipulation (3D displacements). The setup shown in Figure 7a is based on the use of an array of 64 transducers, in an 8x8 square configuration. Each transducer is connected to a control board managed by a software that communicates with the board via an Arduino MEGA. All assembly was performed at CNR-IPCF as part of this project. The ultimate goal is to build a hybrid opto-acoustic setup in air to trap particles in a wide size range (millimeters to micrometers) compared to that achievable with a single technique.

To perform a correct calibration of the acoustic forces, an imaging system was implemented to image the trapped particle by a digital camera. In this way, it is possible to observe the particle fluctuation and to evaluate its dimensions, Fig. 7b. Using static and dynamic calibration methodologies we are able to both measure the force constants of the trap and also provide an estimate of the air resistance coefficient. The static method is based on the position of the particle oscillating around the equi-

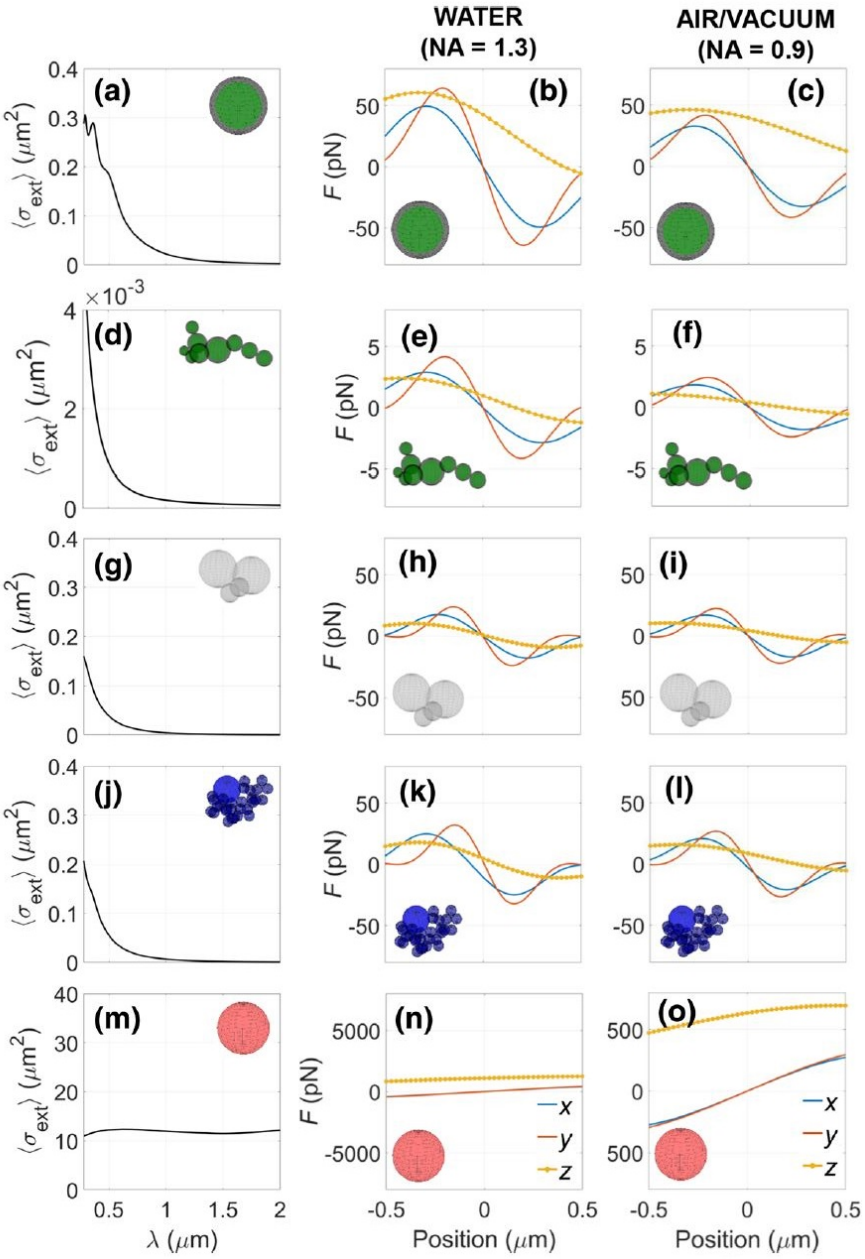

Fig. 6. Extinction cross sections, $\langle\sigma_{ext}\rangle$, and optical trapping force, F, components along x (blue line), y (red line), and z (yellow dots) when the particle is trapped in water (center column) or in air (right column). a–c) Results related to the olivine-aliphatic carbon core-shell sphere. d–f) Calculations for the olivine-aliphatic carbon core-shell cluster. g–i) Quenched melt silica. j-l) Results for the bunch-of-grape carbon Ca-rich. m–o) Results for the TP2 sphere. For the optical trapping calculations, the laser power is fixed at 50 mW and the wavelength at 0.83 μm. Reproduced under Creative Commons license (Polimeno et al., 2021).

librium point of the trap, when subjected to a random perturbation. The dynamic one consists in moving the particle in a controlled way from the trap focus studying the damped oscillations of the particle's position. The experimental calculated force constants Fig. 7(b, c) were then compared with the acoustic trapping forces calculated on the basis of the Gor'kov potential, obtaining a good match (Marrara et al., 2023).

The second acoustic tweezers setup built in our laboratory is based on counter-propagating acoustic beams and is more suitable for trapping and investigating cometary analogue samples (Marzo et al., 2017). The TinyLev is a single-axis acoustic levitator made up of 72 ultrasonic transducers arranged in two opposing spherical cap-shaped arrays (Marzo et al., 2017). The transducers emit acoustic waves at 40 kHz with amplitude adjustable via a power system voltage. The transducers in the same array emit acoustics waves in phase and the phase difference between the signals emitted by the two arrays can be controlled. In such a way, a standing wave can be formed in the space between the arrays, and trapping can be achieved in its nodes. Furthermore, by adjusting the phase difference between the two arrays, the traps can be collectively moved along the vertical direction.

Acoustic forces on spherical particles with sizes smaller than the acoustic wavelength (approximately 8.6 mm in air) can be calculated using the Gor'kov model (Bruus, 2012; Jackson & Chang, 2021). Calculations for styrofoam particles suspended in air showed good agreement between theoretical estimations and experimentally measured acoustic forces (Marrara et al., 2023). By adapting the Gor'kov potential to different gaseous media and levitated particles, it is possible to calculate the acoustic forces on sub-millimeter dust grains in various planetary atmospheres.

The TinyLev setup can trap submillimeter particles with density as high as 3.9 g/cm^3 (Marzo et al., 2017), which is particularly interesting when compared to the density of many extraterrestrial particles. On this basis, this technique can be useful in terrestrial curation facilities for minimizing the contamination of material obtained in sample return missions. Additionally, when combined with a Raman spectrometer, it can be used for mineralogical characterization.

6. Conclusions and outlook

Space tweezers, *i.e.* tools for the contactless trapping and manipulation of particles, can be used to trap and characterize extraterrestrial particulate matter. In recent years, versatile, stable, and more compact optical tweezers setups have been built that have been used to trap micro- and nanoparticles in controlled laboratory experiments. The successful trapping of cosmic dust particles in water is the first step toward the realization of trapping in air–vacuum. This can be achieved using counter propagating beams to reduce the destabilizing effects of radiation pressure, a totally non-invasive micromanipulation method allowing investigation of cosmic dust in a laboratory environment that closely resembles its original conditions in space. Moreover, acoustic tweezers can be used to levitate in air millimeter samples, broadening the size range of particles that can be trapped and manipulated. These methods enable non-destructive, noncontact, and non-contaminating investigation of extraterrestrial particles that can open the way to single-grain characterization, currently difficult with the instrumentation used in space missions. The contactless and noninvasive characterization of planetary dust is expected to provide information on the astrophysical origin, geologic evolution and possible biosignature of their parent bodies. Spectroscopic investigation is expected to have a crucial importance for biohazard assessment for constrained sample return missions. This hope for future space applications shows some experimental challenges that need still to be faced: controlling the particle capture and its storage; developing specific protocols to characterize the trapped particulate matter; improving trapping stability for non-symmetric particles. On the contrary, their use for preliminary characterization of cosmic dust in controlled environments or curation facilities is certainly more at hand.

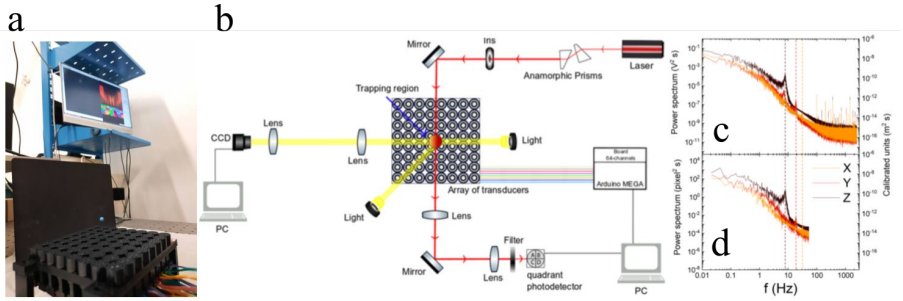

Fig. 7. a) Holographic acoustic tweezers setup. The flat array of acoustic transducers is controlled by a PC in order to create a trapping configuration for the blue polystyrene particle (about 3 mm) which is levitated in air. A dedicated software drives the transducers allowing the manipulation of the particle in the spatial range defined by the array. b) Experimental scheme for the calibration of acoustic tweezers based on the combination of video calibration and the detection of the particle shadow by a four-quadrant photodiode (QPD). c) Power spectrum of the spontaneous particle oscillations along x, y, z of a levitated particle recorded on the QPD and; d) Power spectrum of the signals obtained from the video camera. From the peak frequencies it is possible to obtain the force constants of the trap. Modified under Creative Commons license from (Marrara et al., 2023).

Authors
L. Folco[6,7], O. M. Maragò[1]

Affiliations
[6] Dipartimento di Scienze della Terra, Università di Pisa, Pisa, Italy
[7] CISUP, Center for Instrument Sharing of the University of Pisa, Università di Pisa, Italy

Acknowledgements. We acknowledge financial contribution from the agreement between Agenzia Spaziale Italiana (ASI) and Istituto Nazionale di Astrofisica (INAF) n.2018-16-HH.0, project "SPACE Tweezers" and PRIN 2022 Cosmic Dust II (project number 2022S5A2N7).

References

Abbas, M., Tankosic, D., Craven, P., et al. 2007, Planetary and Space Science, 55, 953
Alali, H., Gong, Z., Videen, G., et al. 2020, Journal of Quantitative Spectroscopy and Radiative Transfer, 255, 107249
Ashkin, A., Dziedzic, J. M., Bjorkholm, J. E., & Chu, S. 1986, Optics letters, 11, 288
Borghese, F., Denti, P., & Saija, R. 2007, Scattering from model nonspherical particles: theory and applications to environmental physics (Springer Science & Business Media)
Bronte Ciriza, D., Magazzù, A., Callegari, A., et al. 2022, ACS photonics, 10, 234
Brownlee, D., Tsou, P., Anderson, J., et al. 2003, Journal of Geophysical Research: Planets, 108
Brownlee, D. E. 1985, Annual Review of Earth and Planetary Sciences, 13, 147
—. 2016, Elements, 12, 165
Bruus, H. 2012, Lab on a Chip, 12, 1014
Calura, F., Pipino, A., & Matteucci, F. 2008, Astronomy & Astrophysics, 479, 669
Colangeli, L., Lopez-Moreno, J., Palumbo, P., et al. 2007, Space Science Reviews, 128, 803
Collareta, A., D'Orazio, M., Gemelli, M., Pack, A., & Folco, L. 2016, Meteoritics & Planetary Science, 51, 351
Davidson, J., Busemann, H., & Franchi, I. A. 2012, Meteoritics & Planetary Science, 47, 1748
Della Corte, V., Rietmeijer, F. J., Rotundi, A., & Ferrari, M. 2014, Astrobiology, 14, 694
Della Corte, V., Palumbo, P., Rotundi, A., et al. 2012, Space Science Reviews, 169, 159–180

Donato, M., Hernandez, J., Mazzulla, A., et al. 2014, Nature communications, 5, 1
Donato, M., Mazzulla, A., Pagliusi, P., et al. 2016, Scientific reports, 6, 31977
Draine, B., Henning, T., Grün, E., & Steinacker, J. 2009, in ASP Conf. Ser, Vol. 414, 453
Draine, B. T. 2003, Annual Review of Astronomy and Astrophysics, 41, 241
Fazio, A., Folco, L., D'Orazio, M., Frezzotti, M. L., & Cordier, C. 2014, Meteoritics & Planetary Science, 49, 2175
Floss, C., Stadermann, F. J., Bradley, J. P., et al. 2006, Geochimica et Cosmochimica Acta, 70, 2371
Folco, L., Cordier, C., et al. 2015, EMU Notes in Mineralogy, 15, 253
Frank, D. R., Westphal, A. J., Zolensky, M. E., et al. 2014, Meteoritics & Planetary Science, 49, 1522
Genge, M. J., Engrand, C., Gounelle, M., & Taylor, S. 2008, Meteoritics & Planetary Science, 43, 497
Gieseler, J., Gomez-Solano, J. R., Magazzù, A., et al. 2021, Advances in Optics and Photonics, 13, 74
Gillibert, R., Balakrishnan, G., Deshoules, Q., et al. 2019, Environmental science & technology, 53, 9003
Gittes, F., & Schmidt, C. F. 1998, Optics letters, 23, 7
Gong, Z., Pan, Y.-L., Videen, G., & Wang, C. 2018, Journal of Quantitative Spectroscopy and Radiative Transfer, 214, 94
Huck, C., Tzschoppe, M., Semenyshyn, R., Neubrech, F., & Pucci, A. 2019, Physical Review Applied, 11, 014036
Iatì, M. A., Giusto, A., Saija, R., et al. 2004, The Astrophysical Journal, 615, 286
Iatì, M. A., Saija, R., Borghese, F., et al. 2008, Monthly Notices of the Royal Astronomical Society, 384, 591
Irrera, A., Magazzù, A., Artoni, P., et al. 2016, Nano letters, 16, 4181
Jackson, D. P., & Chang, M.-H. 2021, American Journal of Physics, 89, 383
Jones, P. H., Maragò, O. M., & Volpe, G. 2015, Optical tweezers: Principles and applications (Cambridge University Press)
Lauretta, D., Balram-Knutson, S., Beshore, E., et al. 2017, Space Science Reviews, 212, 925
Lauretta, D., Adam, C., Allen, A., et al. 2022, Science, 377, 285
Lewis, R. S., Ming, T., Wacker, J. F., Anders, E., & Steel, E. 1987, Nature, 326, 160
Lodders, K., & Amari, S. 2005, Geochemistry, 65, 93
Mackinnon, I. D., & Rietmeijer, F. J. 1987, Reviews of Geophysics, 25, 1527
Magazzú, A., Spadaro, D., Donato, M., et al. 2015, Rendiconti Lincei, 26, 203
Magazzù, A., Ciriza, D. B., Musolino, A., et al. 2022, The Astrophysical Journal, 942, 11
Marrara, S., Ciriza, D. B., Magazzù, A., et al. 2023, IEEE Transactions on Instrumentation and Measurement
Marzo, A., Barnes, A., & Drinkwater, B. W. 2017, Review of Scientific Instruments, 88, 085105
Marzo, A., Seah, S. A., Drinkwater, B. W., et al. 2015, Nature communications, 6, 8661
Mishchenko, M. I., Travis, L. D., & Lacis, A. A. 2002, Scattering, absorption, and emission of light by small particles (Cambridge university press)
Polimeno, P., Magazzu, A., Iati, M. A., et al. 2018, Journal of Quantitative Spectroscopy and Radiative Transfer, 218, 131
Polimeno, P., Magazzù, A., Iatì, M. A., et al. 2021, The European Physical Journal Plus, 136, 1
Rauf, K., Hann, A., Wallis, M., & Wickramasinghe, N. 2010, Int. J. Astrobiology, 9, 183
Rietmeijer, F. J. 1998, Planetary materials, 36, 28
—. 2001, Planetary and Space Science, 49, 71
Rotundi, A., Baratta, G., Borg, J., et al. 2008, Meteoritics & Planetary Science, 43, 367
Saija, R., Cecchi-Pestellini, C., Iatì, M. A., et al. 2005, The Astrophysical Journal, 633, 953
Saija, R., Iatì, M. A., Borghese, F., et al. 2001, The Astrophysical Journal, 559, 993
Saija, R., Iatì, M. A., Denti, P., et al. 2003, Applied optics, 42, 2785
Svak, V., Brzobohatỳ, O., Šiler, M., et al. 2018, Nature communications, 9, 5453

Taylor, A., Baggaley, W., & Steel, D. 1996, Nature, 380, 323

Taylor, S., Messenger, S., & Folco, L. 2016, Elements, 12, 171

Testa Jr, J. P., Stephens, J. R., Berg, W. W., et al. 1990, Earth and planetary science letters, 98, 287

Watanabe, S., Hirabayashi, M., Hirata, N., et al. 2019, Science, 364, 268

Westphal, A. J., Stroud, R. M., Bechtel, H. A., et al. 2014, science, 345, 786

Woosley, S., & Weaver, T. A. 1995, The evolution and explosion of massive Stars II: Explosive hydrodynamics and nucleosynthesis, Tech. rep., Lawrence Livermore National Lab., CA (United States)

Woosley, S. E., Heger, A., & Weaver, T. A. 2002, Reviews of modern physics, 74, 1015